

Optimising the European transmission system for 77% renewable electricity by 2030

ISSN 1752-1416

Received on 30th March 2015

Revised on 23rd October 2015

Accepted on 12th November 2015

doi: 10.1049/iet-rpg.2015.0135

www.ietdl.org

Tom Brown^{1,2} ✉, Peter-Philipp Schierhorn¹, Eckehard Tröster¹, Thomas Ackermann¹

¹Energynautics GmbH, Robert-Bosch-Straße 7, Darmstadt 64293, Germany

²Frankfurt Institute for Advanced Studies (FIAS), Johann Wolfgang Goethe Universität, Ruth-Moufang-Straße 1, 60438 Frankfurt am Main, Germany

✉ E-mail: tom@nworbmot.org

Abstract: To spur Europe to meet ambitious CO₂ emission reduction targets, Greenpeace has developed scenarios for each country to increase its electricity generation from renewable sources. Energynautics was commissioned by Greenpeace to model and optimise the grid extensions in Europe necessary to integrate these large shares of renewables (77% of the total electricity supply by 2030, including 53% from wind and solar). The results and further analysis of the data are presented here. It was found that by preferring high voltage direct current rather than alternating current network extensions, the overall grid upgrades in Europe (measured as the length of new transmission lines) can be reduced by a third. By allowing a small amount of curtailment of variable renewable sources, a disproportionately large number of the necessary grid extensions can be avoided. In addition, the accuracy of decoupling active from reactive power flows is analysed.

1 Introduction

Greenpeace has developed Energy [R]evolution scenarios for all the major countries of the world to make the transition from fossil fuels and nuclear power to renewable energy sources, such as wind and solar [1]. The scenarios consist of technology-specific targets for each country for each decade up to 2050. Using previous versions of the Energy [R]evolution targets for Europe, Energynautics was commissioned by Greenpeace in 2009 [2] and in 2010 [3] to examine the transmission grid upgrades necessary to incorporate the renewables targets for Europe, which aimed for 68% renewable generation in Europe by 2030 and 97% by 2050 (in 2014 renewables coverage was just 32%). Grid upgrades are necessary not just to transport power from the regions where wind and solar resources are best, but also to leverage the smoothing effects seen at the continental scale [4, 5].

Since 2010 much has changed: wind and particularly photovoltaics (PV) have become cheaper, storage technologies have become more viable and the nuclear accident at Fukushima has brought renewables into sharper focus for both policymakers and the public. Greenpeace has updated their Energy [R]evolution technology-specific capacity targets for each European country accordingly, so that 77% of Europe's electricity consumption is covered by renewables by 2030. In 2013 Greenpeace commissioned a new study from Energynautics under the name powE[R] 2030 to examine the grid upgrades required for this level of renewables. The new study was published in 2014 [6] and its results are described in this paper.

Three scenarios were modelled for both 2020 and 2030: an Energy [R]evolution scenario, based on a continent-wide switch to renewables; a reference scenario, representing business as usual; and a conflict scenario, to illustrate what would happen if France, the Czech Republic and Poland were to keep operating large fleets of coal and nuclear power plants inflexibly, while the rest of Europe makes the transition to renewables. In particular, the conflict scenario examined the system conflict if France seeks to increase the capacity factors of its nuclear plants, ramping down as infrequently as possible, thus forcing Germany to curtail generation peaks from PV that it would otherwise export.

In this paper we examine the modelling behind the Energy [R]evolution scenario in 2030 in more detail. The rationale behind

the network technology choices is explained with reference to variations made to the initial basis calculation in order to minimise the necessary grid expansion.

Much research has already been carried out on the benefits that extensions to the transmission grid bring when integrating renewables in the European context. Some of the models used in the literature simplify the power flow in AC networks to a transport model [7, 8] or strongly aggregate the transmission grid [7, 9, 10] for computational efficiency. At the other extreme, the modelling and contingency testing that the European Network of Transmission System Operators for Electricity (ENTSO-E) performs on their Ten Year Network Development Plan (TYNDP) [11] is so detailed that the simulations take a long time and are difficult to iterate repeatedly with new and innovative technologies.

The modelling presented in this paper is novel because it strikes a balance between accurately representing the power flows in the transmission network, while simplifying some assumptions so that new technology options can be prototyped and optimised in an efficient manner (see Section 2.2). We look at the advantage batteries installed in combination with PV units can bring by reducing network overloading during PV peaks, the benefits of ENTSO-E's TYNDP against a more ambitious continent-spanning overlay network using high voltage direct current (HVDC), and the interplay between curtailment and grid expansions. To further test the robustness of the modelling, the consequences of linearising the AC load-flow equations in the optimisation are analysed.

2 Methodology

On the basis of generation capacities determined by Greenpeace for each European country for the year 2030, Energynautics simulated every hour of a full year, using weather data from 2011, to calculate the necessary grid expansions in Energynautics' model of the European transmission system.

2.1 Model input data

Greenpeace provided the capacities of each generation technology and the yearly electrical demand for each country in 2030. The

Table 1 Generating capacities (in GW) by technology for some European countries in the Energy [R]evolution 2030 scenario

Country	Onshore wind	Offshore wind	PV	CSP	Other sources
Czech Republic	4	0	12	0	13
France	62	36	48	1	62
Germany	40	24	90	0	70
Great Britain	30	20	15	0	70
Italy	18	8	40	4	81
Poland	17	10	16	0	35
Spain	55	9	25	68	46
Europe Total	349	145	370	75	594

generation capacities for a selection of European countries in the Energy [R]evolution 2030 scenario are summarised in Table 1; details for the capacities in other countries and yearly generation in TWh/a can be found in [1, 6]. Notable differences compared with today include a commitment to renewables from France and Poland, and 68 GW of concentrated solar power (CSP) in Spain.

Solar technology is dominated by PV; only Spain has more than a few GW of CSP. The heat from the working fluid of CSP is assumed to be storable, so that CSP can be treated as dispatchable within the constraints of the solar energy provided by daily direct insolation.

Regarding general storage availability, besides existing pumped hydroelectric plants it is assumed in some variations of the basic scenario that batteries with a nominal power equal to 10% of the PV nominal power at each network node are installed in 2030.

The capacities from Greenpeace for each generation technology and each country are distributed across the 200 aggregated nodes in Energynautics' grid model of Europe (see Fig. 2) according to technology-specific distribution keys for each country. The distribution keys follow the distribution of existing power plants for conventional generation sources. For wind and solar the distribution in each country is determined by a weighting that takes equal account of the capacity factor at each node and the available land area around each node. The distribution of the load in each country follows the population statistics for Eurostat's NUTS regions.

2011 was chosen as the representative year from which the load and weather data were taken for the simulations. Hourly load figures for each country were downloaded from the ENTSO-E website and scaled linearly according to the demand for 2030. Hourly time series for the availability of wind at each node were generated based on reanalysis wind speed data at 10 m height for Europe from the NOAA Climate Prediction Center [12]. The wind speeds were scaled up to a hub height of 120 m using the formula

$v_1 = v_0 \ln(h_1/r) / \ln(h_0/r)$ from [13], where h_i are the heights, v_i are the velocities and r is the surface roughness. The wind speeds were converted to available power per unit of nominal power using the power curves developed for a typical wind power plant in 2030 from the Tradewind study [14]. Hourly time series for the availability of PV for each node were derived from insolation reanalysis data from Helioclim [15], assuming that the panels were crystalline silicon and in a fixed orientation tilted towards the south at the optimal angle for yearly energy production (between 31° and 42° for the European nodes).

To simulate the power flows in the European transmission network, Energynautics' detailed model of the high voltage grid was used. The grid model has been developed since 2009 and was derived from openly-available data following the methodology outlined in [16]. The model contains 200 aggregated nodes covering the ENTSO-E area (comprising the EU member states, the remaining Balkan countries, Norway and Switzerland). The nodes were chosen to represent all major load and generation sites and all major substations where multiple transmission lines converge. The nodes are connected with over 400 aggregated high voltage alternating current (HVAC) lines that represent all the AC lines at or above 220 kV between the nodes and all the existing HVDC lines (see Fig. 2). ENTSO-E's TYNDP from 2012 [11], split into mid- and long-term projects, can be included as desired. The model can perform both a full AC load-flow or a linearised load-flow, in which active and reactive power flows decouple.

2.2 Grid extension optimisation

The inputs (initial network capacities and impedances, generation capacities and availability time series) were fed into Energynautics' optimal power flow (OPF) program ENAPLAN, which has been developed in-house to optimise power plant dispatch so that necessary grid extensions are minimised. Grid extensions are necessary both to absorb VRE generation that has priority feed-in and to meet the load at every hour.

Here the general approach and theoretical background is given before the algorithm is explained step-by-step.

2.2.1 Theoretical background: Optimising transmission extensions is a difficult problem for several reasons, two of which are discussed in detail here.

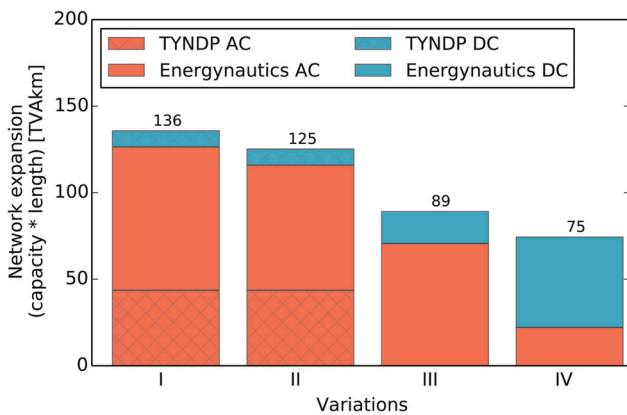


Fig. 1 Network expansion in the variations of the Energy [R]evolution 2030 scenario. The extensions are split up into AC (red) and DC (cyan) and we distinguish between extensions due to TYNDP (hatched) and extensions determined by Energynautics during the optimisation (non-hatched). Network extensions are determined by adding up for each line its length multiplied by the new capacity

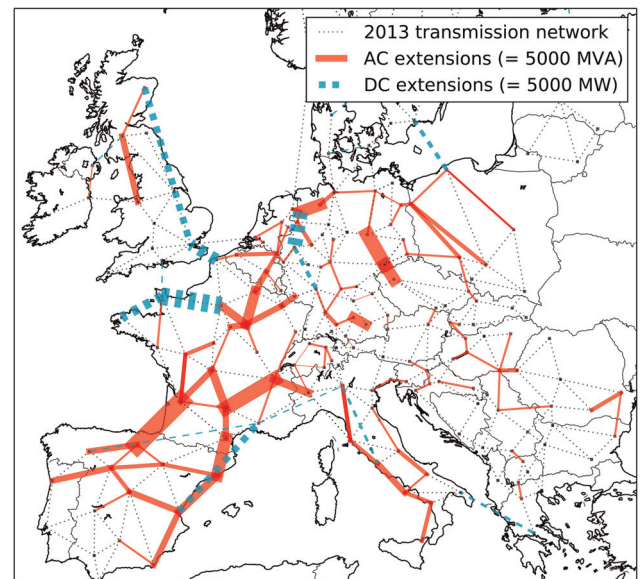


Fig. 2 Network extension map in Variation III (starting from today's network with more HVAC than HVDC). Dark thick red lines represent AC extensions, proportional to the capacity of the extension up to 14 GVA; similarly the dashed cyan lines represent HVDC extensions up to 13 GW. (Background graphic of Europe from Natural Earth [28].)

The first reason is the non-linear nature of the AC load-flow equations and their non-linear dependence on the transmission line capacities, which makes optimisation computationally expensive. Literature surveys of optimal transmission system expansion can be found in [17–19]; new methodologies are also under active development [20]. Here we use a methodology developed in [21] in which linearised power transfer distribution factors (PTDFs) are used to represent the AC load-flow equations, so that they can be used in a linear optimisation program. The PTDFs are then iteratively updated as transmission capacity is increased in the optimisation. A similar methodology was also used in [22].

The nodal PTDFs are equivalent to a linearised AC load-flow calculation, which is often referred to as a ‘DC’ load-flow [23]. To linearise the AC load-flow equations, several simplifying assumptions are made: voltage angles are assumed to be small, voltage magnitudes are all fixed to the nominal voltage, thermal losses are neglected and reactive power flows are ignored. This allows the power flow on the line p_ℓ to be expressed as a linear function of the nodal power imbalances p_i by the PTDF matrix

$$p_\ell = \sum_i \text{PTDF}_{\ell i} p_i \quad (1)$$

The derivation of the PTDF matrix elements in terms of the line series reactances x_ℓ can be found in [21, 23, 24]. The linearisation of the AC load-flow equations can reduce the accuracy of the load-flow; this issue is examined in more detail in Section 3.6.

Another disadvantage of the PTDF formulation is the non-linear dependence of the PTDF on the line characteristics. As additional parallel circuits are added to each line ℓ , the series inductive reactance x_ℓ decreases. The dependence of the PTDF on the x_ℓ is highly non-linear, hence it is not straightforward to optimise the line capacities in a linear program.

To deal with this problem the PTDFs are treated as constant in each OPF step and then if the OPF determines that the line capacity must be increased, the PTDF is updated and the OPF is run again, following the iterative approach of [21]. In [21] it was determined that for this class of problems, the procedure is convergent. The methodology follows the successive linear programming approach introduced by Griffith and Stewart [25].

The load-flow of the HVDC lines is modelled by a source at the to-node coupled to a sink at the from-node. The HVDC power dispatch is independently controllable by the OPF.

A second reason that optimising transmission extensions is difficult is the need to consider as many representative load-flow situations as possible when determining the optimal grid extensions. In principle, the optimisation problem should optimise the grid extensions for all hours of several years simultaneously, to capture as many possible load and weather situations as possible, but this is computationally infeasible given current technology. Some research groups have developed methodologies to select typical hours for the optimisation [7, 21, 22]; for this study a different approach was developed.

2.2.2 Grid extension algorithm: In the approach presented here, the OPF was performed for each hour of the representative year (2011) separately and the PTDF was updated after each step according to the grid extensions determined in that step. The algorithm is now summarised step-by-step:

1. The basic data inputs to the algorithm are the initial network capacities and impedances (based e.g. on today’s network), the capacities for each generation technology at each node and time series for the load and wind and PV availability for each node.
2. Continuous linear OPF calculations are performed sequentially for each hour of the representative year to determine the additional grid extensions for that hour which are necessary so that no lines are overloaded. The exact equations of the OPF are defined below. The variables of the optimisation are the power plant dispatch and the expansion of each transmission line’s capacity. The objective of the optimisation is to minimise the necessary grid extensions

for that hour. The cost of the extension of each line is proportional to its length and takes account of difficult terrain, such as mountainous areas which are costly to traverse.

3. The extension to each line determined by the OPF for a given hour is a continuous number in MW. If this continuous number is greater than 10% of the capacity of an additional circuit, then the capacity of the line is extended by a discrete circuit and the impedance is updated. If the continuous extension is less than 10% then the upgrade is ignored, to avoid upgrades for only slight overloading. 380 kV lines are extended with a capacity of 1500 MVA per circuit and HVDC lines in steps of 1000 MW.
4. If the impedances were updated for the given hour, the PTDF is recalculated.
5. The new PTDF and new line capacities form the basis network for the OPF in the next hour of the year.
6. Once the OPF has been performed for each hour of the year, the OPF is repeated for each hour of the year with the final network configuration from the first run through the year.

The disadvantage of this algorithm is that by performing the optimisation separately for each hour, the algorithm cannot consider many different load-flow situations simultaneously when determining the optimal grid extensions. This is mitigated by only extending the lines above a certain buffer, so that grid extensions are not triggered when the line is overloaded by less than 10% of the capacity of a new circuit.

The algorithm may also converge to different solutions depending on the ordering of the hours which are simulated or based on small changes in the initial conditions. This is a particular concern in the central meshed area of the European grid, where there are many similar options to extend grid capacity. Based on tests during the study that varied the initial conditions, there were only very small changes in the results. A definitive proof of this uniqueness is not provided here, but a likely reason for the uniqueness is that the grid extensions are driven by variable renewable feed-in at the extremities of the European network, where there are only a small number of different grid extensions from which to choose.

The algorithm shows strong convergence to the optimal solution for each run through the representative year. In the final Variation IV of the Energy [R]evolution scenario presented in Section 3.4, the additional grid extensions (measured in MVAkm) in the second run through the year amounted to just 1.8% of the total grid extensions in the first run. Further runs through the representative year showed no additional grid extensions. (There is no continuous incremental convergence because each line is extended in discrete circuits; therefore the algorithm terminates on a final discrete answer.)

2.2.3 OPF equations: The mathematical equations obeyed by the OPF are now described. The OPF program optimises the dispatch $d_{g,i,t}$ of each generation technology g at each node i for each point in time t and the extension P_ℓ of each HVAC line ℓ and P_h of each HVDC line h with the following objective function, which is minimised

$$f(d_{g,i,t}, P_\ell, P_h) = \sum_{g,i} c_g d_{g,i,t} + \sum_\ell c_\ell P_\ell + \sum_h c_h P_h \quad (2)$$

c_g is the marginal cost in €/MWh of the generation technology g and c_ℓ and c_h are the line capacity extension costs in €/MW, which are summarised in Table 2. All costs correspond to prices from 2014 and inflation until 2030 is ignored.

Table 2 Transmission line investment costs

Asset	Unit	Cost
AC overhead line	€/MVAkm	445
DC overhead line	€/MWkm	400
DC submarine	€/MWkm	1100
DC converter pair	€/MW	150,000

The minimisation of the objective function is subject to the following constraints

$$D_{g,i} \geq D_{g,i,t} \geq d_{g,i,t} \geq \hat{D}_{g,i,t} \quad (3)$$

$$\hat{P}_h + P_h \geq |p_{h,t}| \quad (4)$$

$$s(\hat{P}_\ell + P_\ell) \geq |p_{\ell,t}| = \left| \sum_i \text{PTDF}_{\ell i} p_{i,t} \right| \quad (5)$$

$$p_{i,t} = \sum_g d_{g,i,t} + \sum_{h^i} p_{h^i,t} - \ell_{i,t} \quad (6)$$

$$\sum_i p_{i,t} = 0 \quad (7)$$

Here $D_{g,i}$ is the installed capacity of technology g for node i (pre-determined by Greenpeace), $D_{g,i,t}$ is the available active power at time t (which for wind and PV is weather-dependent) and $\hat{D}_{g,i,t}$ is the minimum dispatch (relevant e.g. for renewables with priority feed-in). \hat{P}_ℓ and \hat{P}_h are the pre-existing capacities of the HVAC and HVDC lines, respectively. $p_{h,t}$ and $p_{\ell,t}$ are the power flows in the lines at time t and $\text{PTDF}_{\ell i}$ is the PTDF that determines the AC power flow, following (1). s is a global safety factor for HVAC lines, which reduces the usable thermal capacity of the lines to allow for $n-1$ security and additional loading due to reactive power flows. Here s is set to 70%. $p_{i,t}$ is the net power balance at each node, which consists of the exogenous load $\ell_{i,t}$, the generation dispatch and the sum of the power p_{h^i} HVDC line h^i ending at node i . In this simplification of the model we have omitted additional equations for storage assets, which have efficiency losses and whose energy storage capacity is limited.

Note that the optimisation of the objective function (2) is performed separately for each hour, hence the intention is not to balance the grid extension costs against the dispatch costs for each hour. The grid extension costs are several orders of magnitude higher than the hourly dispatch costs, so that the minimisation of the grid expansion is the priority of the OPF. The dispatch costs are included in the objective function simply to ensure that the dispatch follows the correct merit order. PV and wind have zero price; other generation assets are given a price to determine their position in the merit order.

2.3 Model output data

The outputs of the optimisation include:

- The necessary network extensions and costs.
- Dispatch per node of each generation technology, including curtailment for variable renewables and load factors for controllable generators.
- The network active power flows for HVAC and HVDC lines.

3 Results

Here, the results of the grid optimisation of the Greenpeace Energy [R]evolution scenario for 2030 are presented. In Sections 3.1–3.4, four different variations of the scenario are discussed, in which the parameters of the optimisation are adjusted to reduce the total network extensions. Table 3 shows the different parameter choices for the variations and Fig. 1 charts the total network extensions required to today's transmission network, measured in TVAkM for

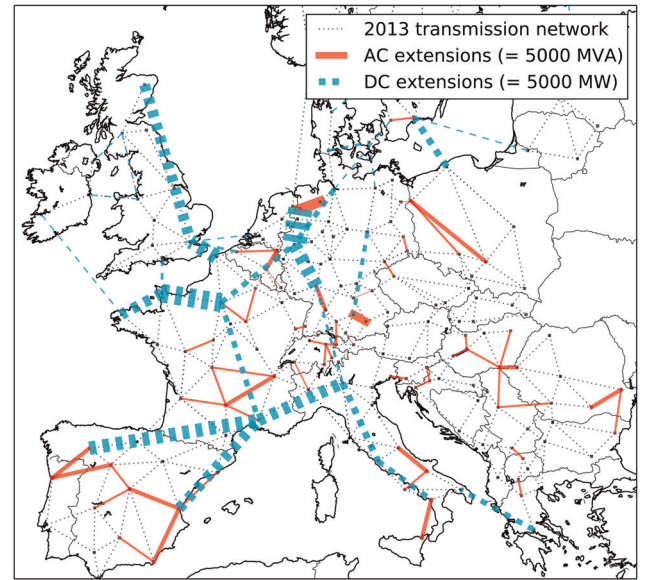


Fig. 3 Network extension map in the final Variation IV (with more HVDC than HVAC). Dark thick red lines represent AC extensions, proportional to the capacity of the extension up to 8 GVA; similarly the dashed cyan lines represent HVDC extensions up to 17 GW. (Background graphic of Europe from Natural Earth [28].)

each variation. The TVAkM measure is determined by adding up for each line its length multiplied by the new capacity.

Reductions in the necessary network expansions in the initial Variation I (Section 3.1) were achieved by installing batteries for some PV systems in Variation II (Section 3.2); by ignoring the ENTSO-E TYNDP projects and optimising European grid extensions based on today's network using an HVDC overlay network in Variation III (Section 3.3); and by building HVDC in preference to HVAC in the final Variation IV (Section 3.4). The final network extensions in Variation IV are shown in Fig. 3.

In addition to the four variations, other aspects of the modelling are examined in the remaining two sections. The trade-off between curtailment and grid extensions is examined in Section 3.5. (In all variations, curtailment of wind and solar was allowed down to 60% of their nominal power at each grid node.) In Section 3.6 the impact of using a full AC load-flow calculation is considered.

3.1 Variation I: basic

In the first variation of the Energy [R]evolution 2030 scenario, it was assumed that all planned projects in ENTSO-E's TYNDP will be built by 2030 and further network extensions were calculated on top of the TYNDP network (the TYNDP is discussed further in Section 3.3). The total network extensions required amounted to 136 TVAkM, of which 61% were the already-planned TYNDP projects. The remaining additional extensions were calculated to be required for Greenpeace's 2030 scenario using the methodology described in Section 2.2. No additional HVDC lines were built beyond those planned in the TYNDP, because the TYNDP HVDC lines were determined by the algorithm to be sufficient and no further HVDC topologies were offered to the algorithm to extend.

Table 3 Variations of the Energy [R]evolution 2030 scenario

Variation	PV batteries	Include TYNDP	HVDC overlay	Prefer HVDC	Network extensions [TVAkM]	Network extension costs [billion Euro]
I	no	yes	no	no	136	72
II	yes	yes	no	no	125	67
III	yes	no	yes	no	89	54
IV	yes	no	yes	yes	75	61

3.2 Variation II: PV batteries

In the second variation batteries were added to 10% (by nominal power) of the PV systems in 2030, to reflect current trends towards increasing self-consumption of distributed energy generation. 370 GW of PV are installed in the scenario, hence 37 GW of batteries were installed, proportional to the PV capacity at each node. The batteries were assumed to have an energy storage capacity corresponding to 2 h at nominal power, so that the storage capacity totalled 74 GWh. The batteries had a total round-trip efficiency of 85% and were operated to reduce the midday PV peak as much as possible by storing the energy and then feeding it back in over 6 h in the evening. By capping the high PV feed-in, which can locally overload the network, the PV batteries reduced the network extensions by around 10% and saved network extension costs of €5.0 billion.

If lithium ion batteries are used, it can be conservatively assumed that the cost of the batteries will be around €150/kWh in 2030 (not adjusted for inflation), based on a literature survey for electric vehicle batteries [26]. If we assume the batteries have a lifespan of 20 years and chain the purchase of the batteries over the 40-year lifespan of the network infrastructure, then the cost of the batteries over 40 years is €15.3 billion, discounted at a yearly rate of 5%. This is three times the cost of the reduced transmission network expansion and therefore seems unfavourable. However, there are other benefits from batteries, including better integration of PV at the distribution network level and the provision of ancillary services such as reactive power for voltage control and variable active power output for frequency control.

3.3 Variation III: PV batteries minus TYNDP plus HVDC overlay

The ENTSO-E publishes a biennial TYNDP. The TYNDP lists all new grid projects planned by the national Transmission System Operators (TSOs) and analyses them in a pan-European context. The 2012 edition [11] comprises 50,000 km of new HVAC and HVDC transmission lines at a cost the European TSOs put at €104 billion (using the cost assumptions from Table 2 we come to only €58 billion; the difference arises from the costs of obtaining land rights, building permissions, etc., which we do not consider here). ENTSO-E tested these planned projects against a scenario with a total of 400 GW of wind and PV in Europe (compared with the 860 GW in the Greenpeace scenario for 2030).

The first two variations started from the assumption that all projects in the TYNDP will be built. The network was then extended as necessary from this basis.

In Variation III the network extension algorithm was run starting from today's network instead of the TYNDP and allowing the algorithm to build an optimised long-distance overlay HVDC grid. The overlay HVDC network connects major European load centres and areas with lots of renewables (see the cyan lines in Fig. 3). The algorithm can expand each line separately with different capacities, or choose not to build the line at all.

The topology of the HVDC overlay network was determined following the methodology in [27] by finding the configuration which would most reduce the flows in the HVAC network, measured in MWkm, for a representative selection of time snapshots. The following important corridors were identified for the HVDC overlay:

1. Scotland to South England.
2. Spain to France.
3. South Italy to North Italy.
4. The French north coast to Paris.
5. North Germany to the Ruhr and/or South Germany.
6. France to Germany.
7. Italy to Germany.

It was found that in Variation III the total network extensions could be reduced by a further 40%. The geographical distribution of the grid expansions in this variation can be found in Fig. 2.

Comparing this variation directly to the TYNDP, it was possible to achieve more than double the renewables integration with our network expansions for a similar investment level (860 GW of wind and PV integrated with network upgrades costing €54 billion, compared with 400 GW in the TYNDP at a cost of €58 billion). This would seem to imply that the TYNDP projects are not ideally optimised for a future with large shares of wind and solar, and with large international power transfers.

One explanation for the difference between our results and the TYNDP is that we optimise using a fully international approach, while ENTSO-E has taken and collected the network extension plans of the national TSOs in the ENTSO-E area and aggregated them. Although there is a focus in the TYNDP on solving international cross-border bottlenecks, particularly with HVDC, our network planning is international in scope from the very start.

Some of the goals of the network expansion in the TYNDP are also not necessarily oriented towards renewables, focussing instead on market integration for conventional generation. In addition, the assumptions behind the modelling are likely to be different: the TYNDP has a different geographical distribution of renewables around Europe, the TSOs may use stricter $n-1$ criteria and in particular they allow much less curtailment, which can lead to significantly higher network expansions (see Section 3.5 and Fig. 4 of this paper).

3.4 Variation IV: PV batteries minus TYNDP plus HVDC overlay with more HVDC

In the first three variations, much less HVDC was built out than HVAC. In the final fourth variation, HVDC was favoured over HVAC (compare the mostly HVAC extensions in Variation III in Fig. 2 with Variation IV in Fig. 3). HVDC was disfavoured in Variations I–III in part due to the high costs of the inverter stations at the ends of each HVDC line (see Table 2). Because the optimisation cannot see all hours of the year at once, due to computation time restrictions, it cannot see the full benefit of the HVDC lines over the year, despite their higher cost. To circumvent this problem, the cost of HVDC in the optimisation was successively reduced to encourage more HVDC; an optimisation cost 75% below the real cost yielded the lowest overall network extensions in TVAkM. With this higher share of HVDC, overall network extensions decreased by 19% between Variation III and IV, measured in terms of line capacities multiplied by length (see Fig. 1). The extension costs (evaluated now with the real HVDC costs) increased by 13% from €54 billion in Variation III to €61 billion in Variation IV, due to the high inverter costs for HVDC. However because HVDC can transport more power for a given mast configuration, the total length of new transmission lines was reduced from 39,000 to

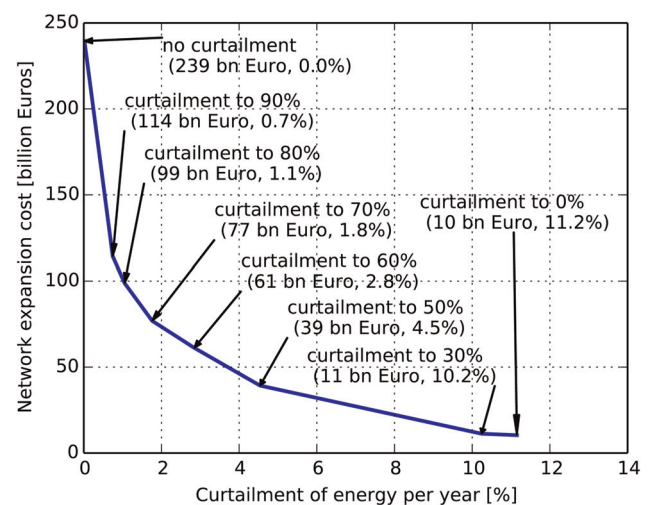


Fig. 4 Results of allowing VRES curtailment down to different fractions of the nominal power of the generating units

26,000 km, a drop of a third. This is a significant advantage, since fewer transmission lines would help to reduce the impact on the landscape and increase public acceptance of new grid infrastructure.

HVDC can reduce network extensions because it channels long-distance power transfers and stops them spreading out in the network ('loop flows') and causing wide areas of the AC network to be built out. HVDC also has other benefits, that become apparent in the tests with the full AC load-flow in Section 3.6: there are lower thermal losses, there is no need for reactive power compensation along the line and there are fewer voltage angle instabilities on AC lines, caused by big power flows over long distance in the AC network.

3.5 Curtailment against grid extensions

In this section the interplay between curtailment and network extensions in the model is examined (see [29] for a similar study for the Iberian peninsula). Although the allowed curtailment level was investigated and fixed at the start of the project, for ease of comparison we present the results from varying curtailment with the configuration used for the final Variation IV (starting from today's grid, PV batteries and more HVDC).

In Fig. 4 the allowed curtailment of wind and solar are varied. The curtailment is controlled by allowing the active power of wind and solar at each node to be reduced to a fixed fraction (e.g. 60%) of the nominal power during hours of high feed-in. This is done by adjusting the minimum dispatch boundary $\hat{D}_{g,i,t}$ in (3). This curtailment is not compulsory, but only happens when the optimisation determines that it can avoid network expansion by reducing the variable renewable sources (VRES) feed-in.

Because VRES reach the highest feed-in levels relatively infrequently, the effect on the loss of energy produced during the year (the x -axis of Fig. 4) can be quite small. However, since the hours of high feed-in cause most of the network expansion as the excess power is transported away, curtailing these rare peaks can significantly reduce the necessary network expansion.

In Fig. 4 this effect can be seen clearly. To absorb every last kWh of wind and solar into the network requires significant network extensions. Curtailing down to just 80% or 70% of the nominal power reduces the necessary expansion by three quarters. On the other hand, if minimal grid extensions are made, there is curtailment to avoid bottlenecks corresponding to 11% of the available energy from VRES. (Even with full curtailment, some network extensions are still necessary, because the Energy [R]evolution scenario for 2030 in Europe has fewer dispatchable generators than today, hence extensions are needed to supply far-away loads in hours when there is no wind or sun.)

The curtailment of VRES causes additional system costs, because the zero-marginal-cost generation of wind and solar must be replaced by other generation sources which may have a non-zero marginal cost. If we assume that the replacement generation has a marginal cost of €50/MWh, then the cost of the curtailment, discounted at a yearly rate of 5% over the 40-year lifespan of the network equipment, can be calculated and compared with the network infrastructure costs. The curtailment and network costs are plotted against each other for different levels of curtailment in Fig. 5. The total costs with unlimited curtailment are high because of the lost VRES generation. The total costs sink as curtailment is restricted, then rise again as unconstrained VRES feed-in drives up the network expansion costs. The minimum total cost is found when curtailment is allowed down to 60% of VRES nominal power, which is why this value was chosen for the simulations.

3.6 DC against AC load-flow

To ensure that the optimisation algorithm is stable and converges within a reasonable time, it uses a linearised load-flow for the AC network, often referred to as a 'DC' load-flow, as described in Section 3.2.

To check that these assumptions are reasonable, the generation dispatch from the optimisation was tested with a full AC load-flow

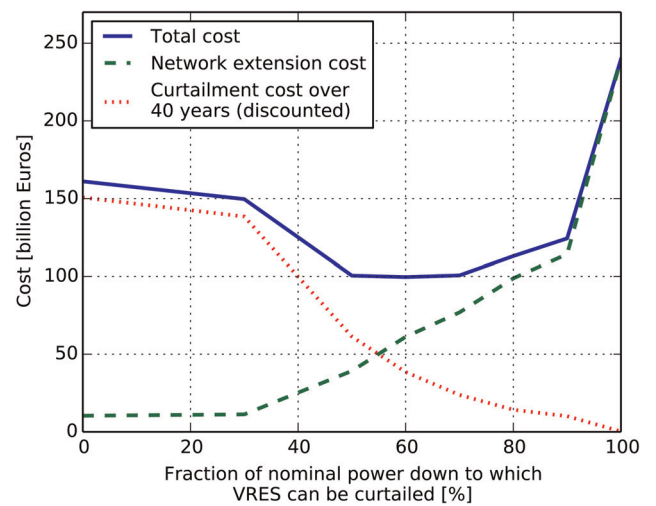


Fig. 5 Interplay between the costs of VRES curtailment (red dotted line) and the network extensions saved by curtailment (green dashed line) as the curtailment level is varied

for each hour of the simulated year. In the AC model, reactive power control is set to keep the voltage magnitude at each node at its nominal value. In addition, some very long lines have series capacitor compensation, to avoid large voltage angles on the lines.

In the AC load-flow, several things can go wrong:

- The load-flow can fail to converge, usually due to voltage angle instability somewhere in the network caused by large power flows on long lines with high impedances.
- Very high thermal losses in the lines can occur, which have to be covered by additional generation.
- High reactive power flows or other distortions due to the redistribution of flows can cause additional loading of transmission lines.

Large voltage angles leading to instability can in most cases be solved by building series compensation into the lines. Voltage instability was not an issue in the final Variation IV with an extensive HVDC overlay network, because the HVDC can take care of the majority of long-distance power transfers. However, in Variation III with more HVAC network extensions, 32% of the snapshots did not converge. This is yet another argument in favour of more HVDC in the European system.

In the final Variation IV the average thermal losses over the year were 10.5 GW in the HVAC network and 1.0 GW in the HVDC network, which in total corresponds to 3.3% of the average load of 352 GW. (HVDC losses were calculated assuming 3% losses over 1000 km, following figures from Siemens [30].) Typical losses in the transmission network are currently in the range of 1.5 to 2.5% [31], hence this figure seems reasonable, once we factor in higher losses due to power being transported over longer distances than today.

When HVAC extensions were preferred in Variation III, the losses were higher at 13.5 GW for the HVAC and 0.4 GW for the HVDC networks, although this was only calculated on the basis of the 68% of snapshots for which the AC load-flow converged; the losses in the non-converging snapshots would likely push this average higher.

The loading of all HVAC lines in all snapshots in the final Variation IV is stacked up in a duration curve in Fig. 6, both from the AC and the 'DC' load-flow. Considering first the DC curve, the loading is limited at 70% to maintain $n-1$ security and allow for extra reactive power flows, which explains the plateau at this value. There is a slight uptick above 70% because brief overloading is allowed to avoid unnecessary grid expansions.

Given that reactive power is provided at each node to keep the voltage at nominal and that thermal losses are low, the difference between AC and DC loading is mostly caused by the reactive power consumption or production of the lines themselves. The

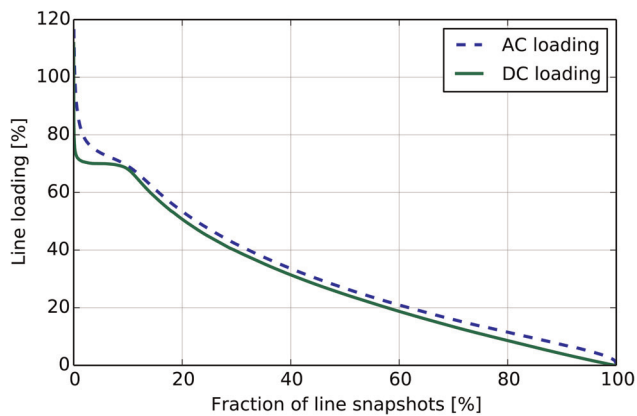


Fig. 6 Loading duration curve for all HVAC lines over all snapshots, comparing results with the full AC load-flow and with the 'DC' load-flow

lines produce reactive power due to their shunt capacitance. This production is proportional to the square of the voltage and remains more or less constant as the loading is increased. The lines consume reactive power due to their series inductance. This consumption is proportional to the square of the current and therefore increases quadratically with the loading. When the loading is low, the line is a net producer of reactive power; at the surge impedance loading (SIL) or natural loading, reactive power is neither produced nor absorbed; above the natural loading, the line is a net consumer of reactive power and this consumption increases quadratically with the loading.

Now we can explain the features of the AC curve in Fig. 6. At low loading, the reactive power production due to the lines' capacitance makes a relatively constant contribution to the loading, which is why the AC curve hovers at a more-or-less constant value above the DC curve. The average SIL in the model is around 60% of the thermal capacity of the lines, and around this value the DC and AC lines come closer. However as the loading increases above 70%, the AC loading increases more strongly, since the reactive power consumption now increases quadratically with the loading. Therefore, at higher loading levels the DC approximation is less accurate, but since the loading was limited to 70% in the DC model, this prevents all but a very few instances where lines go above 100% in individual snapshots in the AC load-flow, and in all but a few cases the AC loading remains below 80%.

These results agree broadly with another study of the accuracy of DC power flow [23], which found that errors were generally of the order of a few per cent, but became worse at high loading.

4 Conclusions

Based on the modelling presented here for Greenpeace's Energy [R] evolution 2030 scenario, a high level of renewables can be integrated into the European power system with only modest changes to the transmission network. With similar investment levels in network infrastructure to those already planned by network operators in ENTSO-E's TYNDP, Europe can cover up to 77% of its electrical load with RES, including up to 860 GW of wind and PV (double the levels considered in the TYNDP) with low curtailment (2.8% of available VRES energy).

By preferring an overlay HVDC grid to continued extension of the HVAC transmission network for long-distance power transfers, the total length of new transmission lines can be reduced by a third (from 39,000 to 26,000 km). This minimises the impact on the landscape and therefore should facilitate public acceptance.

The results remain valid upon the inclusion of the full non-linear AC load-flow equations (at least for the final Variation IV with a high level of HVDC for long-distance power transfers) and can therefore be considered robust and reliable for policymakers considering the low-carbon future of the European power system.

5 Acknowledgments

The modelling for the powE[R] 2030 report [6] was commissioned by Greenpeace International, whom we thank for allowing us to further analyse the results in this paper. Responsibility for the contents of this publication lies solely with the authors.

6 References

- Greenpeace International: 'Energy [R]evolution: A Sustainable World Energy Outlook', available at <http://www.energyblueprint.info/>
- Greenpeace International, EREC: 'Renewables 24/7 Infrastructure Needed to Save the Climate', available at <http://www.greenpeace.org/international/en/publications/reports/renewables-24-7/>, 2009
- Tröster, E., Kuwahata, R., Thomas Ackermann, T.: 'European Grid Study 2030/2050', available at http://www.energynautics.com/downloads/competences/energynautics_EUROPEAN-GRID-STUDY-2030-2050.pdf, 2011
- Huber, M., Dorfner, J., Hamacher, T.: 'Electricity system optimization in the EUMENA region', Munich, 2012, available at <http://mediatum.ub.tum.de/doc/1171502/1171502.pdf>
- Huber, M., Dimkova, D., Hamacher, T.: 'Integration of wind and solar power in Europe: assessment of flexibility requirements', *Energy*, 2014, **69**, pp. 236–246
- Teske, S., Brown, T., Tröster, E., et al.: 'powE[R] 2030: A European Grid for 3/4 Renewable Electricity by 2030', available at <http://www.greenpeace.de/files/publications/201402-power-grid-report.pdf>, 2014
- Czisch, G.: 'Szenarien zur zukünftigen Stromversorgung' (Universität Kassel, 2005)
- Schaber, K., Steinke, F., Mühlich, P., et al.: 'Parametric study of variable renewable energy integration in Europe: advantages and costs of transmission grid extensions', *Energy Policy*, 2012, **42**, pp. 298–508, available at <http://dx.doi.org/10.1016/j.enpol.2011.12.016>
- Becker, S., Rodriguez, R., Andresen, G., et al.: 'Transmission grid extensions during the build-up of a fully renewable pan-European electricity supply', *Energy*, 2014, **64**, pp. 404–418
- Papaemmanouil, A., Tuan, L.A., Andersson, G., et al.: 'A cost-benefit analysis of transmission network reinforcement driven by generation capacity expansion'. Power and Energy Society General Meeting, 2010, pp. 1–8
- ENTSO-E: 'Ten Year Network Development Plan 2012'. Technical Report, European Network of Transmission System Operators for Electricity (ENTSO-E), 2012
- National Center for Environmental Predictions (NCEP): 'NCEP-DOE Reanalysis 2', 2013. Data provided by the NOAA/OAR/ESRL PSD, Boulder, Colorado, USA, from their Web site at <http://www.esrl.noaa.gov/psd/>
- Prandtl, L.: 'The mechanics of viscous flows' (Springer, Berlin, 1935), vol. 3, pp. 34–208
- European Wind Energy Association: 'TradeWind: Integrating Wind: Developing Europe's power market for the large-scale integration of wind power'. Technical Report, 2009
- HelioClim Insolation Database, 2013
- Bialek, J., Zhou, Q.: 'Approximate model of european interconnected system as a benchmark system to study effects of cross-border trades', *IEEE Trans. Power Syst.*, 2005, **20**, pp. 782–788
- Latorre, G., Cruz, R.D., Areiza, J.M., et al.: 'Classification of publications and models on transmission expansion planning', *IEEE Trans. Power Syst.*, 2003, **18**, (2), pp. 938–946
- Wu, F., Zheng, F., Wen, F.: 'Transmission investment and expansion planning in a restructured electricity market', *Energy*, 2006, **31**, pp. 954–966
- Groschke, M., Eßer, A., Möst, D., et al.: 'Neue Anforderungen an optimierende Energiesystemmodelle für die Kraftwerkseinsatz- und Zubauplanung bei begrenzten Netzkapazitäten', *Z Energie*, 2009, **33**, pp. 14–22
- Ahlhaus, P., Stursberg, P.: 'Transmission capacity expansion: an improved transport model'. 2013 4th IEEE/PES Innovative Smart Grid Technologies Europe (ISGT EUROPE), 2013, pp. 1–5
- Hagspiel, S., Jägemann, C., Lindenburger, D., et al.: 'Cost-optimal power system extension under flow-based market coupling', *Energy*, 2014, **66**, pp. 654–666
- Egerer, J., Lorenz, C., Gerbaulet, C.: 'European electricity grid infrastructure expansion in a 2050 context'. 10th Int. Conf. on the European Energy Market, 2013
- Stott, B., Jardim, J., Alsac, O.: 'DC power flow revisited', *IEEE Trans. Power Syst.*, 2009, **24**, (3), pp. 1290–1300
- Grainger, J.J., Stevenson, W.D.: 'Power system analysis' (McGraw-Hill, New York, 2014)
- Griffith, R., Stewart, R.: 'A nonlinear programming technique for the optimization of continuous processing systems', *Manag. Sci.*, 1961, **7**, (4), pp. 379–392
- Nykvist, B., Nilsson, M.: 'Rapidly falling costs of battery packs for electric vehicles', *Nat. Clim. Change*, 2015, **5**, pp. 329–332
- Brown, T., Cherevatskiy, S., Tröster, E.: 'Transporting renewables: systematic planning for long-distance HVDC lines', presented at EWEA 2013 in Vienna
- Background outlines of Europe comes from Natural Earth, free vector and raster map data at <http://naturalearthdata.com>
- Fernandes, C., Frias, P., Olmos, L.: 'Expanding interconnection capacity to integrate intermittent generation in the Iberian Peninsula', *IET Renew. Power Gener.*, 2013, **7**, (1), pp. 45–54
- Siemens: 'UHVDC Transmission System: Benefits', available at <http://www.energy.siemens.com/hq/en/power-transmission/hvdc/hvdc-ultra/#content=Benefits>, 2011
- European Regulators' Group for Electricity and Gas: 'Treatment of Losses by Network Operators: ERGEG Position Paper for public consultation', link to pdf, 2008